Hindawi Publishing Corporation
Journal of Nanomaterials
Volume 2014, Article ID 294350, 9 pages
http://dx.doi.org/10.1155/2014/294350

Research Article

Catalytic Hydrolysis of Ammonia Borane by Cobalt Nickel Nanoparticles Supported on Reduced Graphene Oxide for Hydrogen Generation

Yuwen Yang,[1] Fei Zhang,[1] Hualan Wang,[2] Qilu Yao,[1] Xiangshu Chen,[1] and Zhang-Hui Lu[1]

[1] *College of Chemistry and Chemical Engineering, Jiangxi Normal University, Nanchang 330022, China*
[2] *Department of Information, Yunnan Institute of Technology and Information, Kunming 650224, China*

Correspondence should be addressed to Xiangshu Chen; xiangshuchenjx@126.com and Zhang-Hui Lu; luzh@jxnu.edu.cn

Received 19 February 2014; Accepted 11 March 2014; Published 14 April 2014

Academic Editor: Ming-Guo Ma

Well dispersed magnetically recyclable bimetallic CoNi nanoparticles (NPs) supported on the reduced graphene oxide (RGO) were synthesized by one-step in situ coreduction of aqueous solution of cobalt(II) chloride, nickel (II) chloride, and graphite oxide (GO) with ammonia borane (AB) as the reducing agent under ambient condition. The CoNi/RGO NPs exhibits excellent catalytic activity with a total turnover frequency (TOF) value of 19.54 mol H_2 mol catalyst^{-1} min^{-1} and a low activation energy value of 39.89 kJ mol^{-1} at room temperature. Additionally, the RGO supported CoNi NPs exhibit much higher catalytic activity than the monometallic and RGO-free CoNi counterparts. Moreover, the as-prepared catalysts exert satisfying durable stability and magnetically recyclability for the hydrolytic dehydrogenation of AB, which make the practical reusing application of the catalysts more convenient. The usage of the low-cost, easy-getting catalyst to realize the production of hydrogen under mild condition gives more confidence for the application of ammonia borane as a hydrogen storage material. Hence, this general method indicates that AB can be used as both a potential hydrogen storage material and an efficient reducing agent, and can be easily extended to facile preparation of other RGO-based metallic systems.

1. Introduction

Hydrogen, as a globally accepted clean and environmentally friendly fuel, has attracted widespread research concerns and interests [1]. However, for the widespread use of hydrogen as an energy carrier to achieve sustainable mobility, developing a compact, safe, and affordable means of storing hydrogen remains a major obstacle [2]. Chemical hydrogen storage is thought to be one of the most promising approaches to meet this challenge, because of its considerably high gravimetric and volumetric hydrogen density [3–6]. In recent years, ammonia borane (AB) was discovered as an efficient and safe storage medium for H_2 due to the high capacity (19.6 wt.% and 0.145 kg H_2/L) and stability in ambient atmosphere [7–11]. In the presence of a suitable catalyst, three moles of hydrogen can be released from one mole of AB at room temperature. The hydrolysis of AB can be represented as follows [12–14]:

$$NH_3BH_3\,(aq) + 2H_2O\,(l) \longrightarrow NH_4\,(BO_2)\,(aq) + 3H_2\,(g) \quad (1)$$

So, the discovery of suitable catalysts becomes the main issue of the practical application of AB as an on-board hydrogen medium. With the trend of nanocatalysts applied in the hydrolysis of AB system, transition metal nanoparticles (NPs) catalysts are considered to be a promising option because of their novel structure, electronic properties, and magnetic performances [15–18]. So far, not only nonnoble metal NPs [12, 19–24] and noble metal NPs [13, 20, 25–29], but also their composites [14, 30–38] have been tested for hydrolytic dehydrogenation of AB; among them platinum [20, 25, 26] shows the highest activity. However, concerning

the element abundance and related economic issues, it is clearly a desired goal to prepare low-cost catalysts with high catalytic activity for the terminal practical application of this reaction system in the fuel cell. The catalytic performance of the metal NPs is highly dependent on the dispersion of the active metals. Thus, the aggregation of metal NPs during the catalytic process due to the high surface energies and magnetic properties is the main impediment to restraint their development [36]. To solve this problem, various surfactants and substrates are successfully utilized to obtain catalysts with preferable dispersity [12–14]. Graphene, a single layer of sp^2 carbon lattices, could be an ideal substrate for growing and anchoring metal NPs with good dispersion due to its high specific surface area and large density of free electrons [37–39].

In this work, we have discovered that the CoNi/RGO exhibits excellent catalytic activity in hydrolysis of AB for hydrogen generation. Separation of this catalyst from reactant liquid is quite simple by using a magnet, as CoNi/RGO has an excellent magnetic property. This mild and rapid strategy provides great potential for application of ammonia borane as an on-board hydrogen medium.

2. Experimental

2.1. Graphite Oxide (GO) Preparation. GO was made by a modified Hummers method [40, 41]. Briefly, natural graphite powder (325 mesh) was placed into an 80°C solution of concentrated H_2SO_4 (30 mL), $K_2S_2O_8$ (2.5 g), and P_2O_5 (2.5 g). The mixture was carefully diluted with distilled water and filtered using a 0.2 micron Nylon Millipore filter to remove the residual acid. The product was dried at 80°C under ambient condition overnight. The preoxidized graphite was put into cold concentrated H_2SO_4, then $KMnO_4$ was added gradually under stirring, and the temperature of the mixture was kept below 20°C for 2.5 h. The mixture was stirred at 35°C for 4 h. Afterwards, 250 mL of deionized water was added and the suspension was stirred at 100°C for another 2 h. Subsequently, additional 300 mL of deionized water was added. Shortly after that, 7 mL of 30% H_2O_2 was added to the mixture to terminate the reaction. The suspension was then repeatedly centrifuged and washed first with 5% HCl solution and then with water. Exfoliation of graphite oxide to GO was achieved by ultrasonication of the dispersion for 30 min [42].

2.2. In Situ Synthesis of RGO Supported CoNi NPs (Co/Ni = 0.5/0.5) and Their Catalytic Activities toward the Hydrolysis of AB (Catalysts/AB = 0.05). 8 mL aqueous solution containing $CoCl_2$ (6.01 mg), $NiCl_2$ (6.60 mg), and GO solution (1.77 g containing 0.68‰ GO) was kept in a 25 mL two-necked round-bottom flask. One neck was connected to a gas burette and the other was connected to a pressure-equalization funnel to introduce AB in 2 mL of aqueous solution containing 34.3 mg AB (1 mmol). The reactions were started when the aqueous AB solution was added to the flask with vigorous stirring. The evolution of gas was monitored using the gas burette. After the hydrogen generation reaction was completed, 34.3 mg AB (1 mmol) was added to the flask and the evolution of gas was monitored. A water bath was used to control the temperature of the reaction solution.

For comparison, RGO supported CoNi NPs with different Co/Ni ratio, GO reduced by AB, RGO-free CoNi reduced by AB, and CoNi/RGO reduced by $NaBH_4$ were synthesized using the same method.

2.3. Different Supported Carbon Materials. Sets of experiments with different supported carbon materials (such as activated charcoal and graphite powder) were performed at room temperature. All the experiments were performed in the same way as described in Section 2.2.

2.4. Kinetic Studies of Hydrolytic Dehydrogenation of AB Catalyzed by CoNi/RGO NPs. Temperature was varied at 25°C, 30°C, 35°C, and 40°C, while the ratio of the concentration of CoNi (0.05 mmol) and AB (1 mmol) was kept constant at 0.05 to obtain the activation energy (E_a).

2.5. Stability Test. For stability test, catalytic reactions were repeated 5 times by adding other equivalents of AB (1 mmol) into the mixture after the previous cycle. The molar ratio of catalyst/AB was kept at 0.05.

2.6. Catalyst Characterization. Transmission electron microscope (TEM), energy-dispersive X-ray spectroscopy (EDS), and selected area electron diffraction (SAED) were observed using FEI Tecnai G20 U-Twin TEM instrument operating at 200 kV. Powder X-ray diffraction (XRD) studies were performed on a Rigaku RINT-22005 X-ray diffractometer with a $Cu_{K\alpha}$ source (40 kV, 20 mA). X-ray photoelectron spectroscopy (XPS) measurement was performed with a Thermo ESCALAB 250XI multifunctional imaging electron spectrometer. FTIR spectra were collected at room temperature by using a Thermo Nicolet 870 instrument using KBr discs in the 500–4000 cm^{-1} region. Raman spectrometer was carried out using a confocal Raman microscope (LabRAM HR).

3. Results and Discussion

3.1. Synthesis and Characterization. Chemical reduction methods are widely employed for the synthesis of NPs in solution phase in the presence of surfactant [43], whose presence on the surface diminishes the activity to some extent by blocking some of the active sites when NPs are employed as a catalyst [44]. Surfactant-free NPs are difficult to synthesize because growth of in situ generated nuclei cannot be halted. Herein, RGO supported CoNi NPs were successfully synthesized without using any external surfactant. We employed AB itself (much milder than $NaBH_4$) as the reducing agent in our reactions.

When AB was added to the precursor solution containing $CoCl_2$ and $NiCl_2$ at room temperature, reaction started after an induction period of 55 min, while with the precursor solution with graphene oxide (GO), the induction period time decreased to 3.5 min, as shown in Figure S1 (see Figure S1 in Supplementary Materials available online

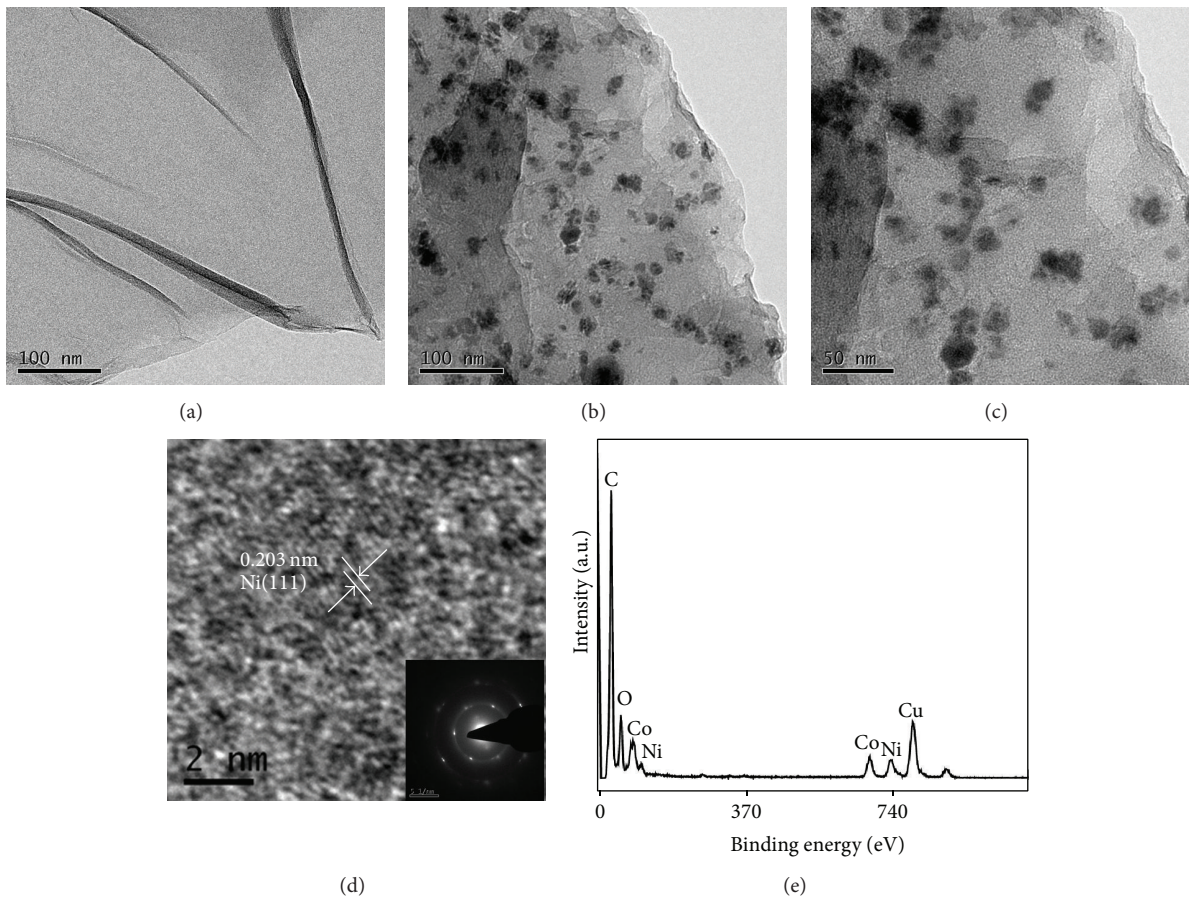

Figure 1: (a) TEM images of GO sheets and (b) and (c) TEM images of CoNi/RGO, (d) HRTEM image of CoNi/RGO, (d inset) SEAD pattern, and (e) EDS spectrum of CoNi/RGO.

at http://dx.doi.org/10.1155/2014/294350/). The decrease of induction period may result from the cooperative effect between RGO and metal NPs, which is mainly caused by the charge transfer across the graphene-metal interface due to the graphene-metal spacing and Fermi level difference. Just before the onset of H_2 evolution, a black colored material was formed. The black powder was RGO supported CoNi NPs (CoNi/RGO).

The microstructures of the CoNi/RGO were characterized by transmission electron microscopy (TEM), high-resolution TEM (HRTEM), energy-dispersive X-ray spectrometer (EDS), and selective area electron diffraction (SAED) (Figure 1). The GO sheets shown in Figure 1(a) are transparent and corrugated together. As shown in Figures 1(b) and 1(c), the NPs were well dispersed on RGO, which helps to prevent the agglomeration. A close examination of the catalysts by HRTEM (Figure 1(d)) indicates that the d-spacing of the particle lattice is ~0.203 nm, which is consistent with the (111) plane of cubic Ni (JCPDS number 04-0850). The EDS spectrum of the specimen shows the presence of Co and Ni (Figure 1(e), which was taken from the specially marked area in the TEM image), with the atomic ratio for Co : Ni being detected to be 0.02 : 0.02, which is in good agreement with the appointed atomic ratio (1 : 1). Therefore, the Co NPs may be in amorphous phase.

Figure 2S shows the power XRD pattern of the Co/RGO and Ni/RGO. The diffraction peak attributed to Ni (111) is observed. However, no diffraction peak of Co exists, which may be caused by the amorphous phase of Co. Therefore, the peak at around 44.10° in the power XRD pattern of the as-prepared CoNi/RGO (Figure 2) corresponds to the Ni (111). Furthermore, the most intense peak at around 11.5° that corresponds to the (001) reflection of GO disappeared and a new peak at around 25.1° is observed in the as-synthesized RGO supported CoNi NPs, indicating that GO is successfully reduced to RGO.

CoNi/RGO was further characterized by X-ray photoelectron spectroscopy (XPS) to investigate the surface nature of the CoNi NPs and RGO (Figure 3). Compared with the peaks of GO (Figure 3(a)), the intensities of oxygen containing functional groups (such as –C–O, –C=O, and –COO) in Co/RGO (Figure 3(b)) decrease significantly, which also reveal the reduction of GO to RGO. Figure 3(c) shows the peaks of Co 2p. There are three peaks whose peak tops are 778.6, 781.7, and 786.0 eV, which stand for zero valent Co and oxidized Co [45]. Figure 3(d) shows the peaks of Ni 2p. There are two peaks at 853.2 and 870.0 eV which are attributed to zero valent Ni, while the other two peaks at 856.6 eV and 874.0 eV stand for oxidized Ni [46]. The formation of the

Table 1: Catalytic activity of different catalysts used for the hydrolytic dehydrogenation of AB.

Catalyst	TOF (mol H_2·mol catalyst^{-1}·min^{-1})	E_a (kJ mol^{-1})	Reference
Ru/γ-Al_2O_3	23.05	67	[27]
CoNi/RGO	19.54	39.89	This work
Ag@CoNi/graphene	15.89	47	[35]
Au@Co	13.64	—	[40]
$Co_{0.32}Pt_{0.68}$/C	10.99	41.5	[31]
Ag@Co/graphene	10.24	20.03	[32]
PSMA-Ni	10.1	38.12	[21]
Cu@Co/graphene	8.36	51.3	[22]
Ag@Ni/graphene	7.7	49.56	[32]
$Co_{0.75}B_{0.25}$	7.24	40.85	[23]
RGO/Pd	6.25	51 ± 1	[28]
Ag/C/Ni	5.32	38.91	[33]
RuCo/γ-Al_2O_3	3.64	47	[34]
Ni/γ-Al_2O_3	2.45	—	[20]
Co/γ-Al_2O_3	2.27	62	[20]

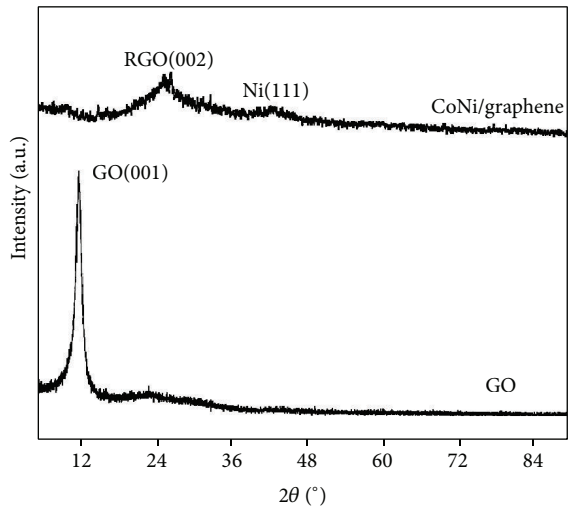

Figure 2: XRD patterns of GO and CoNi/RGO.

oxidized Co and oxidized Ni most likely occurs during the sample preparation process for XPS measurements.

Two peaks centered at 1316 and 1577 cm^{-1} appear in the Raman spectra of the GO and RGO supported CoNi NPs (Figure 4(a)), corresponding to the *D* and *G* bands of the carbon products, respectively. The intensity ratio of the *D* to *G* band (I_D/I_G) is generally accepted to reflect the degree of graphitization of carbonaceous materials and defect density. After loading of the CoNi NPs, the I_D/I_G of GO is increased from 1.14 to 1.61. The relative changes in the *D* to *G* peak intensity ratio confirm the reduction of GO during the in situ fabrication. Figure 4(b) displays the FTIR spectra of GO and CoNi/RGO NPs. After the formation of RGO supported CoNi NPs, the disappearance of C=O peak at 1716 cm^{-1}, C–OH peak at 1399 cm^{-1}, and C–O peak at 1064 cm^{-1} of GO further indicates that the GO was reduced to RGO during the process.

3.2. Catalytic Activities for Hydrolysis of AB. Figure 5(a) shows the composition effect of RGO supported $Co_{1-x}Ni_x$ on AB hydrolysis (x = Co:Co + Ni), with the molar ratio for catalysts to AB being 0.05. Obviously, by changing the molar ratio, the NPs demonstrate different catalytic activities. As a result, $Co_{0.5}Ni_{0.5}$/RGO displays the best catalytic performance in the hydrolysis of AB, generating a stoichiometric amount of hydrogen (H_2/AB = 3.0) in the shortest time (3.07 min) with a turnover frequency (TOF) value of 19.54 mol H_2 mol catalyst^{-1} min^{-1}, which is higher than the most reported nonnoble metal-based NPs and even many noble metal-based NPs, as shown in Table 1, while CoNi/RGO show better activity than pure Co NPs or pure Ni NPs supported on RGO, indicating the positive effect of metal interaction in the bimetallic CoNi NPs on hydrogen generation from hydrolysis of AB. As shown in Figure S3, compared with the NPs reduced by $NaBH_4$, the as-synthesized NPs generated by AB exhibit higher catalytic activities, which confirms that it is possible to achieve much more control over the nucleation and growth process of the RGO by choosing weaker reducing agents.

Figure 5(b) presents the plots of the volume of hydrogen generated from the AB solution versus the reaction time at room temperature in the presence of pure $Co_{0.5}Ni_{0.5}$NPs, GO, and the $Co_{0.5}Ni_{0.5}$/RGO catalysts. No hydrogen generation was observed for GO, suggesting that GO has no catalytic activity for the hydrolysis of AB. The hydrogen productivity from AB catalyzed by pure $Co_{0.5}Ni_{0.5}$NPs is around 49.3% in 79.7 min. However, the activity of Co-Ni/RGO is much higher than that of pure Co-Ni NPs without RGO. The enhanced catalytic activity for AB hydrolysis reaction should result from the cooperative effect between RGO and Co-Ni NPs. Furthermore, to study the effects of the supported carbon materials on the catalytic performances of the as-synthesized bimetallic NPs, $Co_{0.5}Ni_{0.5}$/graphite powder and $Co_{0.5}Ni_{0.5}$/activated charcoal are prepared and their catalytic activities toward hydrolysis of AB are studied. As

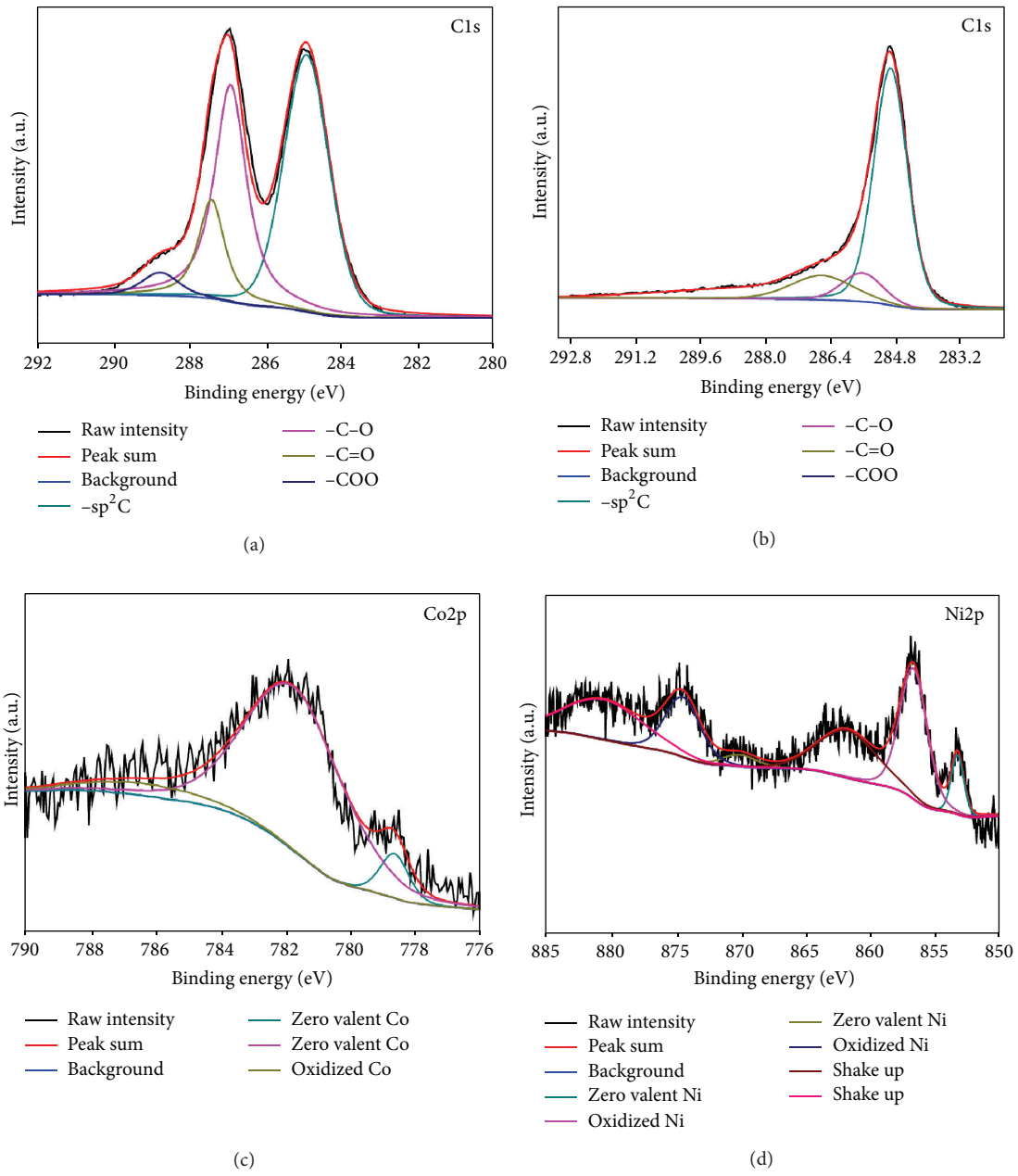

Figure 3: XPS of spectra of ((a) and (b)) C1s of GO and CoNi/RGO, (c) Co2p of CoNi/RGO, and (d) Ni2p of CoNi/RGO.

shown in Figure S4, their catalytic activities are inferior to that of $Co_{0.5}Ni_{0.5}$/RGO NPs, highlighting the dominant factor of RGO in facilitating hydrolysis of AB in our system.

In order to get the activation energy (E_a) of the AB hydrolysis catalyzed by CoNi/RGO NPs, the hydrolytic reactions at different temperatures in the range of 298–313 K were carried out. The values of the rate constant k at different temperatures were calculated from the slope of the linear part of each plot from Figure 6(a). The Arrhenius plot of ln k versus $1/T$ for the catalyst is plotted in Figure 6(b), from which the apparent activation energy was determined to be approximately 39.89 kJ/mol, being lower than most of the reported E_a values (Table 1), indicating the superior catalytic performance of the as-synthesized CoNi/RGO catalysts.

3.3. Reusability and Recycle Ability. The reusability of the catalysts is crucial in the practical application. The recyclability of CoNi/RGO catalysts up to the fifth run for hydrolysis of AB is shown in Figure 7. The as-synthesized CoNi/RGO catalysts retain 68% of their initial activities in the hydrolysis of AB in the fifth run, indicating their superior recycle stabilities. The observed activity loss is likely to result from the precipitation of metaborates to the catalyst surface [19]. Moreover, the in situ synthesized CoNi/RGO

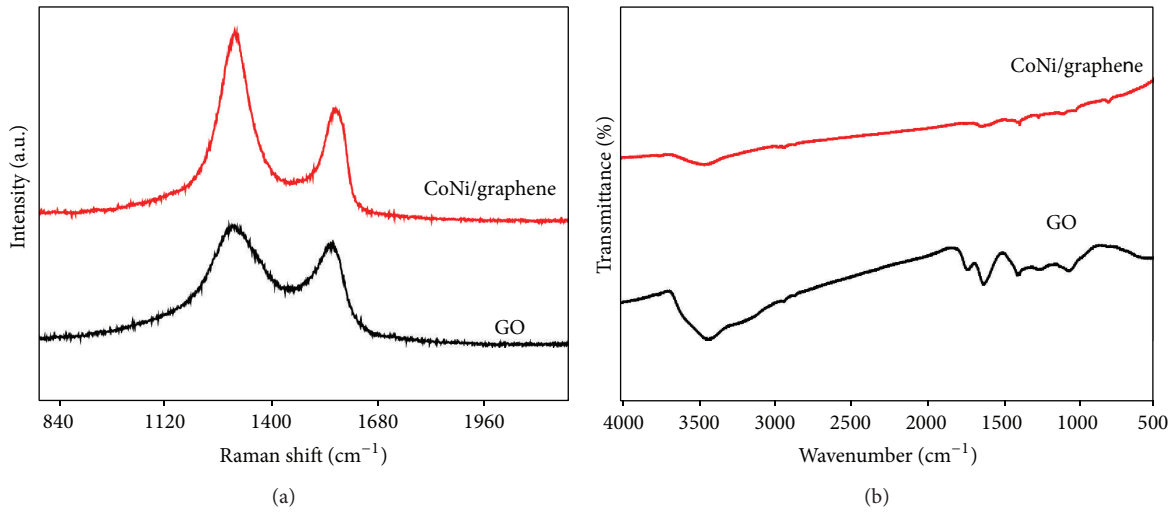

FIGURE 4: (a) Raman spectra and (b) FTIR spectra of the GO and CoNi/RGO.

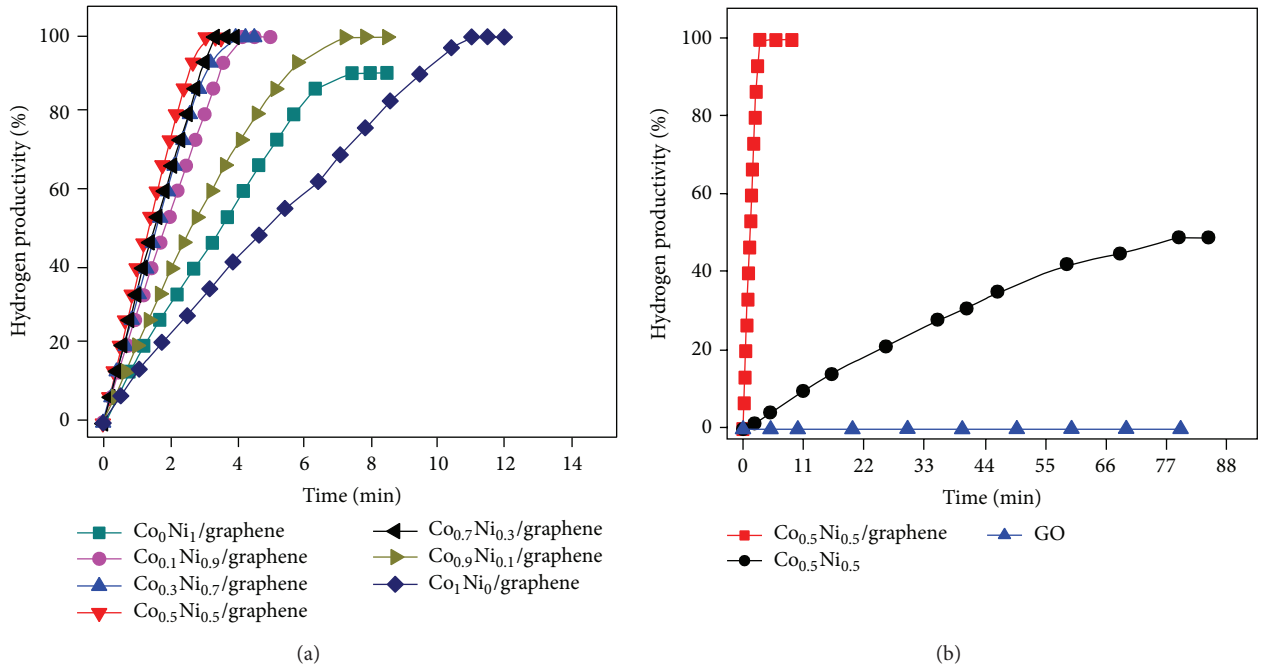

FIGURE 5: Hydrogen generation from hydrolysis of ammonia borane (0.10 M, 10 mL) over (a) the CoNi/RGO catalysts at ambient condition. CoNi/AB = 0.05 (molar ratio) and (b) the $Co_{0.5}Ni_{0.5}$/RGO, $Co_{0.5}Ni_{0.5}$, and GO.

are magnetic and thus can be separated from the reaction solution by an external magnet (Figure 7 inset), which makes the practical recycling application of nanocatalysts more convenient.

4. Conclusion

In summary, we have developed a facial in situ one-step method for the synthesis of magnetic RGO supported bimetallic CoNi NPs using AB as a reductant. The CoNi/RGO exhibit superior catalytic activity, with a turnover frequency (TOF) value of 19.54 H_2 mol catalyst^{-1} min^{-1} and an activation energy (E_a) value of 39.89 kJ mol^{-1}. The RGO supported CoNi NPs exhibit much higher catalytic activity than the graphite powder and activated charcoal supported or monometallic and RGO-free CoNi counterparts. Compared with catalysts reduced by $NaBH_4$, the CoNi/RGO catalysts generated by the milder reducing agent AB exhibit higher catalytic activities. Moreover, the CoNi/RGO catalysts show good durable stability and magnetic recyclability for the hydrolytic dehydrogenation of AB, which makes the practical recycling application of the catalyst more convenient. This simple synthetic method can be extended to other RGO-based bimetallic systems for more application.

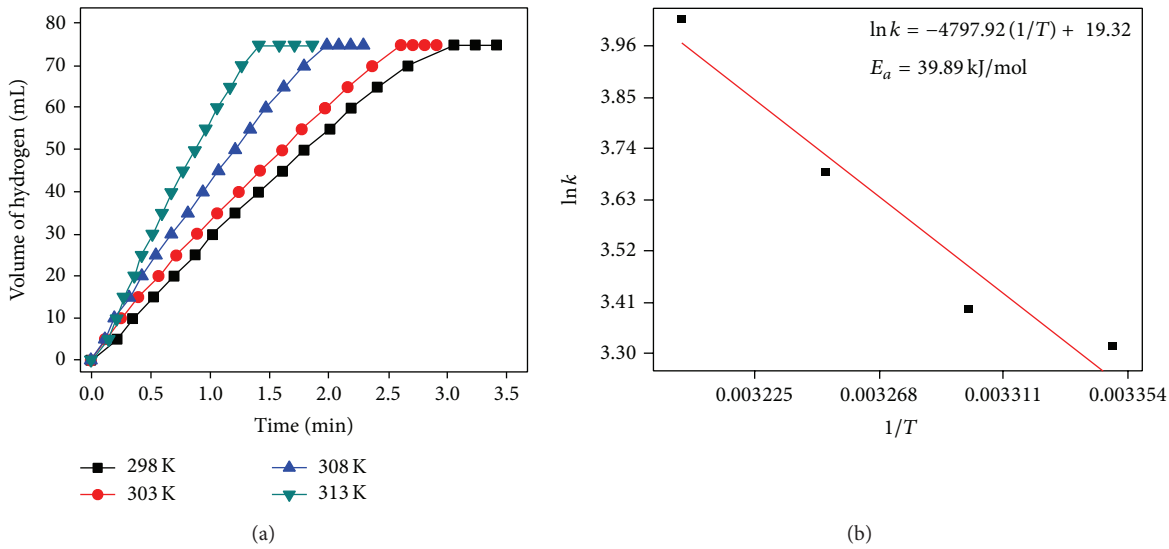

(a) (b)

Figure 6: (a) Plots of volume of hydrogen generated versus time for $Co_{0.5}Ni_{0.5}$/RGO catalyzed hydrolysis of AB at four different temperatures in the range of 298–313 K, CoNi/AB = 0.05 and (b) Arrhenius plot obtained from the data of Figure 6(b).

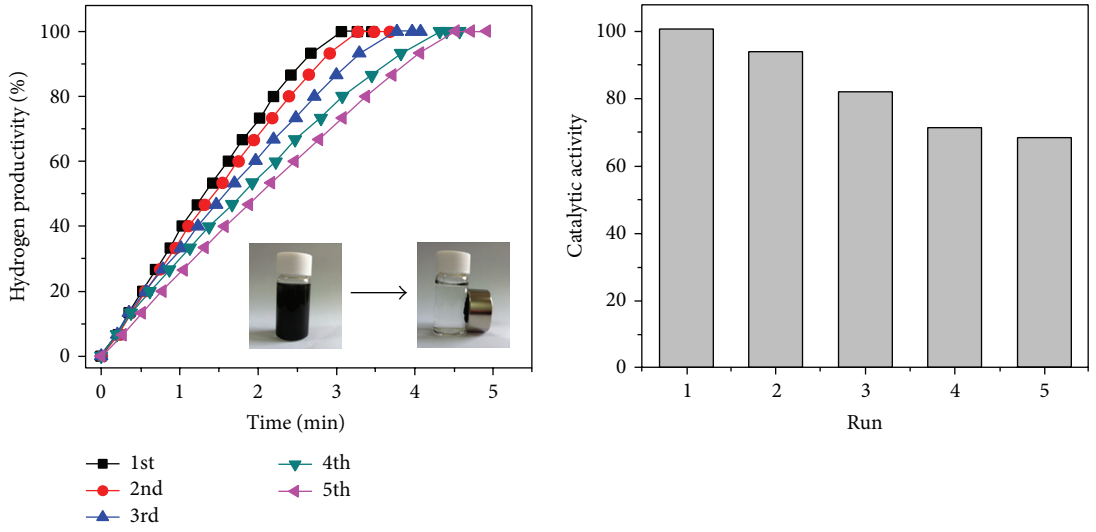

(a) (b)

Figure 7: (a) Hydrogen generation from hydrolysis of ammonia borane (0.10 M, 10 mL) catalyzed by $Co_{0.5}Ni_{0.5}$/RGO from the 1st to 5th cycle, CoNi/AB = 0.05, and (inset) photographs of the $Co_{0.5}Ni_{0.5}$/RGO before (left) and after (right) the magnetic separation; (b) percentage of initial catalytic activity of $Co_{0.5}Ni_{0.5}$/RGO in successive runs after the reuse for the hydrolysis of AB.

Conflict of Interests

The authors declare that there is no conflict of interests regarding the publication of this paper.

Acknowledgments

This work was financially supported by the National Natural Science Foundation of China (no. 21103074), the Natural Science Foundation of Jiangxi Province of China (nos. 20114BAB203010 and 20132BAB203014), Jiangxi Provincial Department of Science and Technology (no. 20111BDH80023), and the Scientific Research Foundation of Graduate School of Jiangxi Province (YC2013-S105). Zhang-Hui Lu was supported by the Sponsored Program for Cultivating Youths of Outstanding Ability in Jiangxi Normal University, the Young Scientist Foundation of Jiangxi Province (20133BCB23011), and "Gan-po talent 555" Project of Jiangxi Province.

References

[1] L. Schlapbach and A. Züttel, "Hydrogen-storage materials for mobile applications," *Nature*, vol. 414, no. 6861, pp. 353–358, 2001.

[2] J. S. Zhang, Y. Zhao, D. L. Akins, and J. W. Lee, "Calorimetric and microscopic studies on the noncatalytic hydrothermolysis of ammonia borane," *Industrial & Engineering Chemistry Research*, vol. 50, pp. 10407–10413, 2011.

[3] U. Eberle, M. Felderhoff, and F. Schüth, "Chemical and physical solutions for hydrogen storage," *Angewandte Chemie International Edition*, vol. 48, pp. 6608–6632, 2009.

[4] J. Yang, A. Sudik, C. Wolverton, and D. J. Siegel, "High capacity hydrogen storage materials: attributes for automotive applications and techniques for materials discovery," *Chemical Society Reviews*, vol. 39, no. 2, pp. 656–675, 2010.

[5] U. B. Demirci and P. Miele, "Chemical hydrogen storage: "Material" gravimetric capacity versus "system" gravimetric capacity," *Energy and Environmental Science*, vol. 4, no. 9, pp. 3334–3341, 2011.

[6] Z. H. Lu, Q. L. Yao, Z. J. Zhang, Y. W. Yang, and X. S. Chen, "Nanocatalysts for hydrogen generation from ammonia borane and hydrazine borane," *Journal of Nanomaterials*, vol. 2014, Article ID 729029, 2014.

[7] Z. H. Lu and Q. Xu, "Recent progress in boron- and nitrogen-based chemical hydrogen storage," *Functional Materials Letters*, vol. 5, Article ID 1230001, 9 pages, 2012.

[8] C. W. Hamilton, R. T. Baker, A. Staubitz, and I. Manners, "B-N compounds for chemical hydrogen storage," *Chemical Society Reviews*, vol. 38, no. 1, pp. 279–293, 2009.

[9] M. Yadav and Q. Xu, "Liquid-phase chemical hydrogen storage materials," *Energy & Environmental Science*, vol. 5, pp. 9698–9725, 2012.

[10] H. L. Jiang and Q. Xu, "Catalytic hydrolysis of ammonia borane for chemical hydrogen storage," *Catalysis Today*, vol. 170, no. 1, pp. 56–63, 2011.

[11] U. B. Demirci and P. Miele, "Sodium borohydride versus ammonia borane, in hydrogen storage and direct fuel cell applications," *Energy and Environmental Science*, vol. 2, no. 6, pp. 627–637, 2009.

[12] S. Akbayrak and S. Özkar, "Ruthenium(0) nanoparticles supported on multiwalled carbon nanotube as highly active catalyst for hydrogen generation from ammonia-borane," *ACS Applied Materials & Interfaces*, vol. 4, pp. 6302–6310, 2012.

[13] J. Wang, Y. L. Qin, X. Liu, and X. B. Zhang, "In situ synthesis of magnetically recyclable graphene-supported Pd@Co core–shell nanoparticles as efficient catalysts for hydrolytic dehydrogenation of ammonia borane," *Journal of Materials Chemistry*, vol. 22, pp. 12468–12470, 2012.

[14] J. M. Yan, Z. L. Wang, H. L. Wang, and Q. Jiang, "Rapid and energy-efficient synthesis of a graphene–CuCo hybrid as a high performance catalyst," *Journal of Materials Chemistry*, vol. 22, pp. 10990–10993, 2012.

[15] L. Kesavan, R. Tiruvalam, M. H. A. Rahim et al., "Solvent-free oxidation of primary carbon-hydrogen bonds in toluene using Au-Pd alloy nanoparticles," *Science*, vol. 331, no. 6014, pp. 195–199, 2011.

[16] R. Ghosh Chaudhuri and S. Paria, "Core/shell nanoparticles: classes, properties, synthesis mechanisms, characterization, and applications," *Chemical Reviews*, vol. 112, no. 4, pp. 2373–2433, 2012.

[17] R. Ferrando, J. Jellinek, and R. L. Johnston, "Nanoalloys: from theory to applications of alloy clusters and nanoparticles," *Chemical Reviews*, vol. 108, no. 3, pp. 845–910, 2008.

[18] R. C. Sekol, X. K. Li, P. Cohen, G. Doubek, M. Carmo, and A. D. Taylor, "Silver palladium core–shell electrocatalyst supported on MWNTs for ORR in alkaline media," *Applied Catalysis B: Environmental*, vol. 138-139, pp. 285–293, 2013.

[19] Z. H. Lu, J. P. Li, A. L. Zhu et al., "Catalytic hydrolysis of ammonia borane via magnetically recyclable copper iron nanoparticles for chemical hydrogen storage," *International Journal of Hydrogen Energy*, vol. 38, pp. 5330–5337, 2013.

[20] Q. Xu and M. Chandra, "Catalytic activities of non-noble metals for hydrogen generation from aqueous ammonia-borane at room temperature," *Journal of Power Sources*, vol. 163, no. 1, pp. 364–370, 2006.

[21] Ö. Metin and S. Özkar, "Water soluble nickel(0) and cobalt(0) nanoclusters stabilized by poly(4-styrenesulfonic acid-co-maleic acid): highly active, durable and cost effective catalysts in hydrogen generation from the hydrolysis of ammonia borane," *International Journal of Hydrogen Energy*, vol. 36, pp. 1424–1432, 2011.

[22] Y. S. Du, N. Cao, L. Yang, W. Luo, and G. Z. Cheng, "One-step synthesis of magnetically recyclable rGO supported Cu@Co core–shell nanoparticles: highly efficient catalysts for hydrolytic dehydrogenation of ammonia borane and methylamine borane," *New Journal of Chemistry*, vol. 37, pp. 3035–3042, 2013.

[23] A. K. Figen, "Dehydrogenation characteristics of ammonia borane via boron-based catalysts (Co–B, Ni–B, Cu–B) under different hydrolysis conditions," *International Journal of Hydrogen Energy*, vol. 38, p. 9186, 2013.

[24] Y. W. Yang, Z. H. Lu, Y. J. Hu et al., "Facile in situ synthesis of copper nanoparticles supported on reduced graphene oxide for hydrolytic dehydrogenation of ammonia borane," *RSC Advances*, vol. 4, pp. 13749–13752, 2014.

[25] M. Chandra and Q. Xu, "Room temperature hydrogen generation from aqueous ammonia-borane using noble metal nanoclusters as highly active catalysts," *Journal of Power Sources*, vol. 168, no. 1, pp. 135–142, 2007.

[26] M. Rakap, E. E. Kalu, and S. Özkar, "Polymer-immobilized palladium supported on TiO_2 (Pd–PVB–TiO_2) as highly active and reusable catalyst for hydrogen generation from the hydrolysis of unstirred ammonia–borane solution," *International Journal of Hydrogen Energy*, vol. 36, pp. 1448–1455, 2011.

[27] G. P. Rachiero, U. B. Demirci, and P. Miele, "Facile synthesis by polyol method of a ruthenium catalyst supported on γ-Al_2O_3 for hydrolytic dehydrogenation of ammonia borane," *Catalysis Today*, vol. 170, no. 1, pp. 85–92, 2011.

[28] P. X. Xi, F. J. Chen, G. Q. Xie et al., "Surfactant free RGO/Pd nanocomposites as highly active heterogeneous catalysts for the hydrolytic dehydrogenation of ammonia borane for chemical hydrogen storage," *Nanoscale*, vol. 4, pp. 5597–5601, 2012.

[29] Q. L. Yao, W. M. Shi, G. Feng et al., "Ultrafine Ru nanoparticles embedded in SiO_2 nanospheres: highly efficient catalysts for hydrolytic dehydrogenation of ammonia borane," *Journal of Power Sources*, vol. 257, pp. 293–299, 2014.

[30] J. M. Yan, X. B. Zhang, T. Akita, M. Haruta, and Q. Xu, "One-step seeding growth of magnetically recyclable Au@Co core-shell nanoparticles: highly efficient catalyst for hydrolytic dehydrogenation of ammonia borane," *Journal of the American Chemical Society*, vol. 132, pp. 5326–5327, 2010.

[31] X. Yang, F. Cheng, Z. Tao, and J. Chen, "Hydrolytic dehydrogenation of ammonia borane catalyzed by carbon supported Co core-Pt shell nanoparticles," *Journal of Power Sources*, vol. 196, no. 5, pp. 2785–2789, 2011.

[32] L. Yang, W. Luo, and G. E. Cheng, "Graphene-supported Ag-based core-shell nanoparticles for hydrogen generation in

hydrolysis of ammonia borane and methylamine borane," *ACS Applied Materials & Interfaces*, vol. 5, pp. 8231–8240, 2013.

[33] M. Wen, B. L. Sun, B. Zhou, Q. S. Wu, and J. Peng, "Controllable assembly of Ag/C/Ni magnetic nanocables and its low activation energy dehydrogenation catalysis," *Journal of Materials Chemistry*, vol. 22, pp. 11988–11993, 2012.

[34] G. P. Rachiero, U. B. Demirci, and P. Miele, "Bimetallic RuCo and RuCu catalysts supported on γ-Al_2O_3. A comparative study of their activity in hydrolysis of ammonia-borane," *International Journal of Hydrogen Energy*, vol. 36, no. 12, pp. 7051–7065, 2011.

[35] L. Yang, G. Cheng, J. Su, W. Luo, and X. Meng, "In situ synthesis of graphene supported Ag@CoNi core–shell nanoparticles as highly efficient catalysts for hydrogen generation from hydrolysis of ammonia borane and methylamine borane," *Journal of Materials Chemistry A*, vol. 1, pp. 10016–10023, 2013.

[36] L. S. Ott and R. G. Finke, "Transition-metal nanocluster stabilization for catalysis: a critical review of ranking methods and putative stabilizers," *Coordination Chemistry Reviews*, vol. 251, pp. 1075–1100, 2007.

[37] X. Huang, X. Y. Qi, F. Boey, and H. Zhang, "Graphene-based composites," *Chemical Society Reviews*, vol. 41, pp. 666–686, 2012.

[38] S. Garaj, W. Hubbard, A. Reina, J. Kong, D. Branton, and J. A. Golovchenko, "Graphene as a subnanometre trans-electrode membrane," *Nature*, vol. 467, no. 7312, pp. 190–193, 2010.

[39] Z.-H. Lu, H.-L. Jiang, M. Yadav, K. Aranishi, and Q. Xu, "Synergistic catalysis of Au-Co@SiO_2 nanospheres in hydrolytic dehydrogenation of ammonia borane for chemical hydrogen storage," *Journal of Materials Chemistry*, vol. 22, no. 11, pp. 5065–5071, 2012.

[40] D. Q. Wu, F. Zhang, H. W. Liang, and X. L. Feng, "Nanocomposites and macroscopic materials: assembly of chemically modified graphene sheets," *Chemical Society Reviews*, vol. 41, pp. 6160–6177, 2012.

[41] W. S. Hummers Jr. and R. E. Offeman, "Preparation of graphitic oxide," *Journal of the American Chemical Society*, vol. 80, no. 6, p. 1339, 1958.

[42] N. I. Kovtyukhova, P. J. Ollivier, B. R. Martin et al., "Layer-by-layer assembly of ultrathin composite films from micron-sized graphite oxide sheets and polycations," *Chemistry of Materials*, vol. 11, pp. 771–778, 1999.

[43] A. Roucoux, J. Schulz, and H. Patin, "Reduced transition metal colloids: a novel family of reusable catalysts?" *Chemical Reviews*, vol. 102, no. 10, pp. 3757–3778, 2002.

[44] D. Astruc, F. Lu, and J. R. Aranzaes, "Nanoparticles as recyclable catalysts: the frontier between homogeneous and heterogeneous catalysis," *Angewandte Chemie International Edition*, vol. 44, no. 48, pp. 7852–7872, 2005.

[45] P. Song, Y. Li, W. Li, B. He, J. Yang, and X. Li, "A highly efficient Co (0) catalyst derived from metal-organic framework for the hydrolysis of ammonia borane," *International Journal of Hydrogen Energy*, vol. 36, no. 17, pp. 10468–10473, 2011.

[46] K. W. Park, J. H. Choi, B. K. Kwon, S. Lee, and A. Y. E. Sung, "Chemical and electronic effects of Ni in Pt/Ni and Pt/Ru/Ni alloy nanoparticles in methanol electrooxidation," *Journal of Physical Chemistry B*, vol. 106, pp. 1869–1877, 2002.